Preprints of the 21st IFAC World Congress (Virtual)
Berlin, Germany, July 12-17, 2020

Detection of Defected Zone Using 3D Scanning Data to Repair Worn Turbine Blades

Edson Kenji Ueda * [1] **Ahmad Barari** ** [4] **Andre K. Sato** * [2]
Marcos S. G. Tsuzuki * [3]

* *Escola Politécnica da Universidade de São Paulo, São Paulo, Brazil. Mechatronics and Mechanical Systems Engineering Department Computational Geometry Laboratory.*
** *University of Ontario Institute of Technology, Oshawa, Canada. Faculty of Engineering & Applied Science.*

Abstract: This work presents a method to determine the curve that approximates the worn perimeter in a turbine blade. A CAD model is used as reference and it is searched for points of a measured point cloud that shows a worn in a blade. A threshold is used to filter measured and fabrication errors, resulting in a point cloud that just indicates the worn region. The alpha complex algorithm is used to triangulate the determined points. The resulting triangulation eliminates long edges making possible to a triangulation with concave regions. The boundary points of this triangulation is determined by the search for edges that belongs to just one triangle. A simulated annealing is used to optimize a cost function to determine the piecewise cubic Bézier curve that approximates these boundary points.

Keywords: Point Cloud, Bézier curve, Piecewise Curve, Curve Fitting, Simulated Annealing, CAD, Digital Twin.

1. INTRODUCTION

The Industry 4.0 is the forth industrial revolution that focus on inter-connectivity, automation, machine learning and real-time data. In this revolution, the incorporation of sensors on-board manufacturing equipment, the easy network accessibility and artificial intelligent algorithm are all combined to obtain the best possible manufacturing process control. One of the majors concepts of the Industry 4.0 is cyber-physical systems (CPS), that is the integration of computation (artificial intelligence algorithms), network, and the physical process. There is a feedback loop process, in which embedded computers affects the physical process and vice-versa thought a network connection.

A component of the CPS is the Digital Twin, that is a replication of the living and the non living physical entities in the virtual world (El Saddik, 2018). These replication enable the communication between the physical and digital world, in which physical and digital entities could exchange data, that can be widely used to optimize the manufacturing process by the use of artificial intelligence algorithms. The replication of an object into digital world (reverse engineering) can be performed with a Coordinate Metrology Machine (CMM), that uses a combination of tactile or contact probes and optical sensors to capture 3D discrete points from an object. There is a problem in these machines, while tactile sensors measure the coordinates with better precision, the measuring speed is slow. On the other hand, the optical sensor can measure the points in a higher speed, but with worst precision. Zhao et al. (2009) develop a method to optimize the inspection path to minimize the inspection time. Lately, with the advent of laser scans, the digitization of objects can be obtained faster and with a huge amount of data.

An application of the Digital Twin is to perform the Deviation Zone Estimation (DZE), in which it is determined the difference of a measured object and the designed object. There are several works on this subject (Schleich et al., 2014), Lalehpour and Barari (2017) developed a method to make quality control of the manufactured work piece, Berry and Barari (2019) developed a method to inspect in real-time the quality of the process of manufacturing, by searching blisters in the painting process, Gohari et al. (2019) developed a method to increase the speed to determine the DZE. All of these works are related to control the manufacturing process by evaluating the final manufacturing workpiece.

This work will use the DZE in preventing maintenance. The DZE is used to determine the worn region of a turbine blade. It is developed a method to determine a representative curve of the worn region perimeter and by monitoring this region, based on that curve a decision can be made on whether or not a repair is necessary. While the points are a discrete representation of the worn region, a curve is a continuous representation of the region, so with the control points of the curve is possible to create a high level model of the worn region, in which it is possible to

[1] email: edson.ueda@usp.br.
[2] email: andre.kubagawa@gmail.com.
[3] email: mtsuzuki@usp.br.
[4] email: Ahmad.Barari@uoit.ca

monitor the length of the perimeter of the region, and if you have a surface model it is also possible to monitor the area and volume of the wear.

This work is structured as follows. In Section 2 a brief overview of some basics concepts, such as, Bézier curve, piecewise Bézier curve and curve fitting are presented. In Section 3, the proposed method is presented. In Section 4, some results are presented and, finally, the conclusions are drawn in Section 5.

2. BASIC CONCEPTS

2.1 Bézier Curve

The Bézier curve is a parametric curve given by

$$\mathbf{P}(u) = \sum_{i=0}^{n} \mathbf{p}_i B_{i,n}(u), \qquad u \in [0,1] \tag{1}$$

where $\mathbf{p}_i$ are the control points, the curve has $n+1$ control points and $B_{i,n}(u)$ is the Bernstein polynomial basis function defined as

$$B_{i,n}(u) = \binom{n}{i} u^i (1-u)^{n-i}, \qquad i = 0, ..., n. \tag{2}$$

where $\binom{n}{i}$ is the binomial function, given by

$$\binom{n}{i} = \frac{n!}{i!(n-i)!} \qquad \binom{0}{0} \equiv 1. \tag{3}$$

2.2 Piecewise Cubic Bézier Curve

Piecewise cubic Bézier curve (see Fig. 1) is used to overcome a property of the the Bézier curve in which each control point modify all the curve, and it is a problem in the curve fitting problem once one control point can change part of the curve in which the fitting is already done. The creation of a piecewise cubic Bézier curve is done by adopting the last control point of a curve segment as the first control point of the following curve segment, and also calculate the second control point of the following curve with the equation

$$\mathbf{p}_{3i+4} = \mathbf{p}_{3i+3} - (\mathbf{p}_{3i+2} - \mathbf{p}_{3i+3}) * \beta_{3i+4}, \tag{4}$$

where j is the number of curve segments minus one, $i = 0, \ldots, j-1$ and $\beta > 0$ is a proportionality factor. Fig. 1 shows an example of a piece-wise curve with 2 cubic Bézier curves, in which $\mathbf{p}_3$ is a connecting control point.

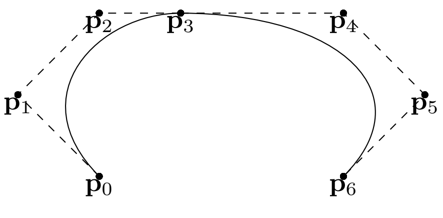

Fig. 1. Piecewise Bézier curve with 2 curves, in which $\mathbf{p}_3$ is a connecting control point.

2.3 Curve Fitting - Curve Approximation

The objective of the curve fitting problem is to determine a curve that approximates or interpolates a sequence of points. The determination of the curve is done by defining control points $(\mathbf{p}_0, ..., \mathbf{p}_n)$ that ensure the desired characteristic. In the approximation problem the curve has to pass near the sequence of points, while in the interpolation problem the curve has to pass through the sequence of points. The cost function to be minimized is

$$\begin{aligned} F(\mathbf{p}_0, ..., \mathbf{p}_n) =& W \cdot \sum_{k=1}^{m} |\mathbf{d}_k - \mathbf{P}(u_k)|^2 \\ &+ (1-W) \cdot len(\boldsymbol{P}(u)) \end{aligned}, \tag{5}$$

with $\mathbf{p}_0, ..., \mathbf{p}_n$ being the $n+1$ control points to be determined, $\mathbf{d}$ the sequence of $m+1$ points and $len(\boldsymbol{P}(u)$ the length of the determined curve (P).

Eq. 5 determines the curve that approximates a sequence of points. Note that this equation consists of two parts, the first is the discrepancy between the sequence of points and the approximate curve; and the second is the length of the approximate curve. The minimization of just the first part determines a family of curves with different length and the determination of longer curves is called overfitting. The curve length $(len(\boldsymbol{P}(u))$ is used as regularization to avoid this problem, and it is controlled by the weight W. The minimization of Eq. 5 is done by the adaptive neighborhood simulated annealing (ANSA) developed by (Martins and Tsuzuki, 2006, 2008; Martins et al., 2016), in which the control points of the piecewise cubic Bézier curve are adjusted.

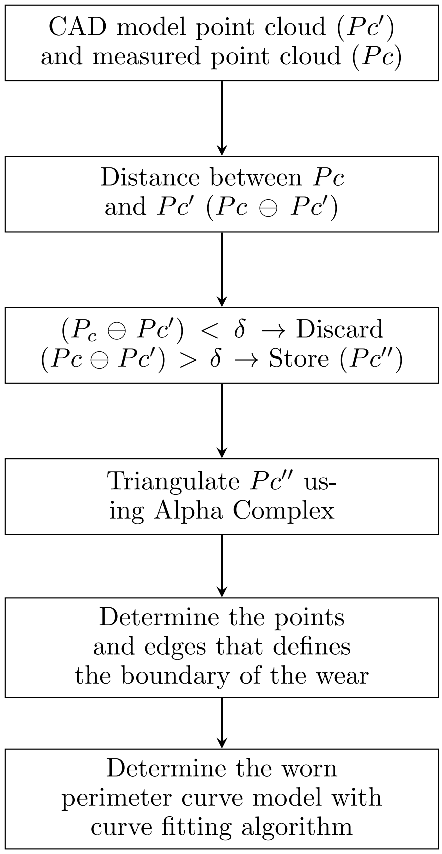

Fig. 2. Flowchart of the proposed methodology.

3. PROPOSED METHOD

The proposed method of this work is presented in the Fig. 2. Two point clouds are used as input data of the method, the first one (Pc') is the objects CAD model point cloud, and the second one (Pc) is the objects measured point cloud, in which the worn region needs to be detected.

The first step of the method consists in determining for each point in Pc the closest point in point cloud Pc' (this operation is represented as $Pc \ominus Pc'$). The determination of the closest point can be performed by calculating the euclidean distance between a point of Pc and all points of Pc' and keep the point with minimum distance. There is a problem in this approach, the cost of this algorithm is $O(n^2)$ and if there is a huge number of points in Pc and Pc' the algorithm will be inefficient. Herein, we use the k-d tree data structure (Bentley, 1975) to find the closest point. This algorithm was used by Takimoto et al. (2016) to make a registration of two point clouds, in which it is necessary to determine the distance between two point clouds. This data structure is a multidimensional binary search tree that divides the space in two half-spaces with a hyper-plane, so in each level it is generated two half-spaces that contains its child nodes, which are recursively subdivided. The search for the nearest neighbour uses one property of the k-d tree to eliminate the search in one half-space in each level. The set of all nearest points defines a new point cloud.

Before explaining the second step for the worn region detection, some definitions are made. In the previous step, for each point from Pc there is a correspondent nearest neighbour point in Pc', and also the distance between these two points. If the difference of both point cloud is just the wear, a Boolean operation can determine it. The Boolean operation is equivalent to the determination of all points from Pc which distance to the corresponding point from Pc' is greater than zero. However, there are at least two other sources of error that can be detected with this naive approach, and it is required to define a threshold. The first error source is the manufacturing error that is the dimensional tolerance of the manufacturing, and the second error source is the sensor measurement error. Then, a filtration is necessary in this step. It is used a threshold of δ as filtration criteria, and if the distance between the point from P_c and its corresponding point from Pc' is smaller that this threshold the point is filtered. The resulting filtered point cloud (Pc'') has the points which define the worn region of the object.

The next step is the triangulation of Pc'' point cloud. The triangulation is performed in 2D, just the x and y coordinates of the points are used in the triangulation. The Alpha complex triangulation algorithm (Edelsbrunner, 1995). This algorithm is similar to the Delaunay triangulation algorithm. The Delaunay triangulation determines circumferences from 3 points in which there are no point inside the determined circumference. Then, in the end all the circumferences determines the triangles of the triangulation. In the alpha complex algorithm, if the radius of the circumference is greater than $1/\alpha$ the triangle is discarded. So, edges with high length are eliminated by modifying α. With this feature it is possible to create triangulations with holes and concave boundaries.

Once the triangulation of the worn region points is performed, the determination of the boundary is simple. The determination of the boundary of a triangulated area happens by searching the edges which are present in just one triangle, and these edges and its respective points are the elements that defines the boundary.

The last step of the method is the determination of the curve that approximates the boundary points. In the previous step, the list of boundary points and its respective edges were determined, it is easy to order these points. First, choose a random starting point and with the list of edges it is possible to find the next point, the following point is found by selecting the previous edge end point as the start of the next edge start point and the edge end point is the third point of the sequence. This procedure is repeated until the first point is found again. Once the boundary points are sequenced it is used (Ueda et al., 2018) a curve fitting algorithm to determine the boundary perimeter representative curve. The cost function to be minimized by the ANSA (Martins and Tsuzuki, 2010; Tavares et al., 2019) to determine the piecewise cubic Bézier curve that approximates the worn points boundary is Eq. 5, and using as an example the curve from Fig. 1 the parameters to be adjusted are

(1) Coordinate x of point $\mathbf{p}_1$ (p_1x)
(2) Coordinate y of point $\mathbf{p}_1$ (p_1y)
(3) Coordinate z of point $\mathbf{p}_1$ (p_1z)
(4) Coordinate x of point $\mathbf{p}_2$ (p_2x)
(5) Coordinate y of point $\mathbf{p}_2$ (p_2y)
(6) Coordinate z of point $\mathbf{p}_2$ (p_2z)
(7) Proportionality factor of point $\mathbf{p}_4$ (β_4)
(8) Coordinate x of point $\mathbf{p}_5$ (p_5x)
(9) Coordinate y of point $\mathbf{p}_5$ (p_5y)
(10) Coordinate z of point $\mathbf{p}_5$ (p_5z)

Note that for every new piece of curve, it is necessary 4 new parameters to represent the new segment to be adjusted by ANSA, these parameters are the x, y and z coordinate of a control point and a proportional factor β.

4. RESULTS

The proposed method was tested with a turbine blade (see Fig. 3). The CAD model was sampled with $3,583,009$ points and the worn blade was created by adding a random noise at $16,193$ points. Fig. 4 shows these points, Fig. 4(a) show the CAD with the wear, and Fig. 4(b) shows with red points the worn location. Note that if the test is performed in a measured object, there are no CAD model, just a point cloud, however to better view the worn region, the image shows the CAD model and not just a point cloud. The creation of the wear was done by applying a random noise at the normal direction in each red point with intensity between $[-1, 0]$.

As mentioned, if there are no errors and noise in the measured point cloud, the detection of the wear is simply performed by a Boolean operation and all the red points are easily detected. The errors and noisy simulation was done with the same procedure of the worn region creation. It was added a random noise to the points at the normal direction, however the intensity was between $[-0.01, 0.01]$ and it was applied to all the points excluding the red points. If a Boolean operation is performed in the noisy point cloud, all the points would have been detected. Then, using as threshold $\delta = 0.01$ as filtration criteria the noise

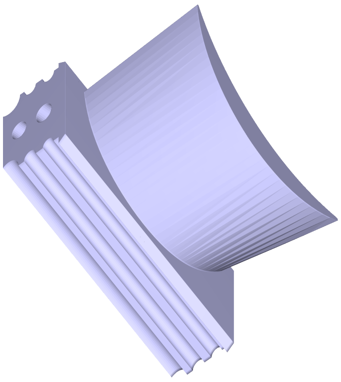

Fig. 3. Turbine blade CAD model.

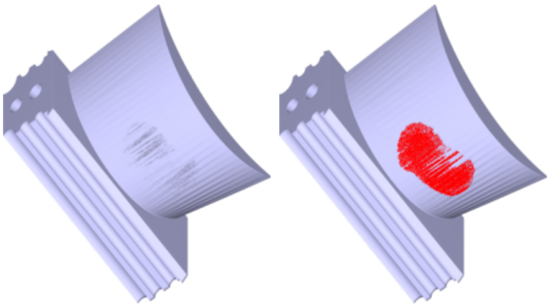

(a) (b)

Fig. 4. Turbine blade created worn region. (a) The wear are in the middle of the blade with a max of 1 random dislocation in the normal direction; (b) worn region points are marked with red points.

were eliminated and the resulting points are shown in Fig. 6, the blue points are the detected worn region points and the red points are the not detected worn region points. It was detected $16,015$ points corresponding 98.9% of the created worn region points. The square distance between two point clouds was used as comparison metric and it is given by Eq. 6,

$$Metric = \sum_{i=0}^{n} (Pc_i'' - Pc_i'*)^2, \tag{6}$$

with n being the number of detected points and $Pc_i'*$ the respective nearest neighbour of each Pc_i''. The difference of the detected points and the created worn region points using Eq. 6 as metric is 0.0065. This value was expected, once just 178 points are not detected and these points max distance are 0.01 leading to a maximum value of 0.0178 for the adopted metric.

Using the blue points from Fig. 6 the alpha complex algorithm was applied with $\alpha = 0.9$. The resulting triangulation is shown in Fig. 7, and note that the concave part of the point cloud in not triangulated, circle with radius more than 1.11 was eliminated resulting the elimination of the long edges. The points and edges of the point cloud is shown in Fig. 8, the red points are the 289 boundary points and the blue line are the edges between these points. The piecewise cubic Bézier curve that approximates the worn perimeter is shown in Fig. 9. Fig. 9(a) are the curve in the X-Y plane and the Fig. 9(b) is in a 3D view, in which is possible to verify that the curve approximates

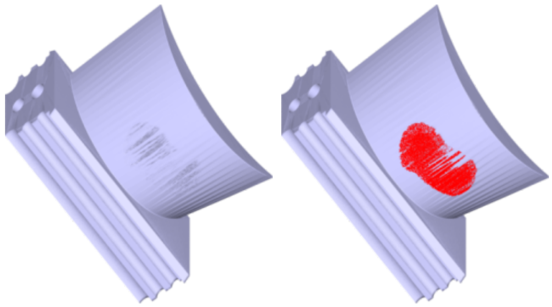

(a) (b)

Fig. 5. Turbine blade with noise, all the points excluding the worn region are added with a max of 0.01 random noise. (a) The worn region are the same of the previous image, however it is possible to see that the there are some noise in the top and base of the blade; (b) worn region points are marked with red points.

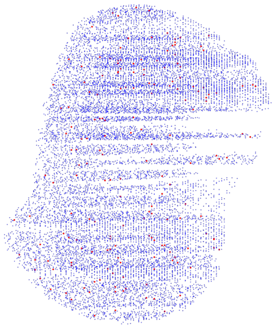

Fig. 6. The blue points are the detected worn region points, and the red points are the not detected worn region points.

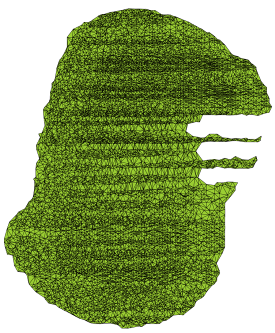

Fig. 7. Triangulation of the detected worn region points using alpha complex with $\alpha = 0.9$.

the Z coordinate. It was used 10 curves to approximate the perimeter, in which its control point are represented with black diamond, the black line are the convex-hull of the curve, the red line the piecewise cubic Bézier and the yellow points the boundary points of the wear.

5. CONCLUSION

It was proposed a method to determine the curve that approximates the perimeter of a worn region of a turbine blade. The detection of the wear from a point cloud was possible by using a threshold as filtration criteria, that represents the manufacturing tolerance and the measuring sensor error. The resulting filtered points are the worn

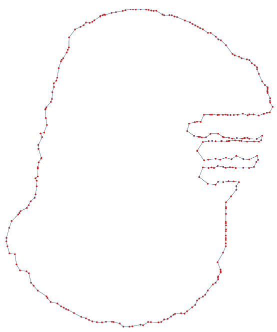

Fig. 8. Boundary of the worn region, the red points are the boundary points and the blue line are the edges linking these points.

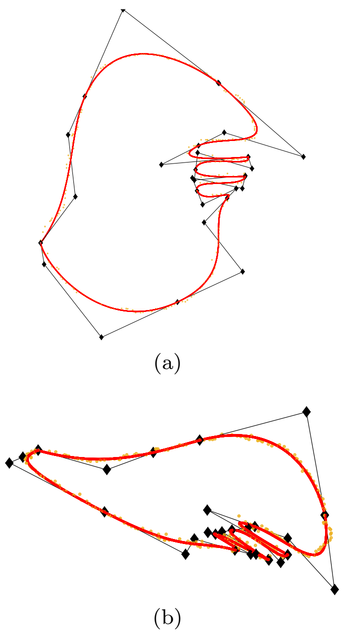

Fig. 9. Piecewise cubic Bézier curve with 10 segments that approximates the perimeter of the wear. Black diamond are the control points, black line the convex-hull of the curve, red line the curve and yellow points the boundary points. (a) $X - Y$ plane; (b) 3D view.

region, and this region boundary are obtained by the search for triangles edges from the region triangulation that are contained at only one triangle. The worn region perimeter was determined from the boundary points using the ANSA to adjust the parameters of a piecewise cubic Bézier curve. The proposed method was successfully tested on a artificially created example, in which the worn region are detected and the perimeter of this region is approximated by a piecewise cubic Bézier curve. This method shows how it is possible to do a preventing maintenance of a turbine blade by making a digital inspection of the blade into the search for worn regions.

The next step is to propose a method to detect multiple worn regions and divide them to be possible to monitor each region individually. Once a method that monitors multiple worn regions is created, it is possible to use the method in real wear cases. Another future works is to develop a method to create a surface from the worn points and calculate the worn region area and volume.

ACKNOWLEDGEMENTS

EK Ueda is supported by CNPq (Grant 140.518/2015-0). MSG Tsuzuki is partially supported by the CNPq (Grants 305.959/2016–6 and 311.195/2019-9).

REFERENCES

Bentley, J.L. (1975). Multidimensional binary search trees used for associative searching. *CACM*, 18, 509–517.

Berry, C. and Barari, A. (2019). Cyber-physical system utilizing work-piece memory in digital manufacturing. *IFAC-PapersOnLine*, 52(10), 201–206.

Edelsbrunner, H. (1995). Smooth surfaces for multi-scale shape representation. In P.S. Thiagarajan (ed.), *Foundations of Software Technology and Theoretical Computer Science*, 391–412. Springer Berlin Heidelberg, Berlin, Heidelberg.

El Saddik, A. (2018). Digital twins: The convergence of multimedia technologies. *IEEE MultiMedia*, 25, 87–92.

Gohari, H., Berry, C., and Barari, A. (2019). A digital twin for integrated inspection system in digital manufacturing. *IFAC-PapersOnLine*, 52(10), 182–187.

Lalehpour, A. and Barari, A. (2017). Developing skin model in coordinate metrology using a finite element method. *Measurement*, 109, 149–159.

Martins, T.C. and Tsuzuki, M.S.G. (2006). Simulated annealing applied to the rotational polygon packing. *IFAC Proc Vol (IFAC-PapersOnline)*, 12(PART 1).

Martins, T.C. and Tsuzuki, M.S.G. (2010). Placement over containers with fixed dimensions solved with adaptive neighborhood simulated annealing. *B Pol Acad Sci-Tech*, 57(3), 273—280.

Martins, T.C. and Tsuzuki, M.S.G. (2008). Rotational placement of irregular polygons over containers with fixed dimensions using simulated annealing and no-fit polygons. *J Braz Soc Mech Sci*, 30, 205–212.

Martins, T.C., Tsuzuki, M.S.G., Camargo, E.D.L.B., Lima, R.G., Moura, F.S., and Amato, M.B.P. (2016). Interval simulated annealing applied to electrical impedance tomography image reconstruction with fast objective function evaluation. *Comput Math Appl*, 72(5), 1230–1243.

Schleich, B., Anwer, N., Mathieu, L., and Wartzack, S. (2014). Skin model shapes: A new paradigm shift for geometric variations modelling in mechanical engineering. *CAD*, 50, 1–15.

Takimoto, R.Y., Tsuzuki, M.S.G., Vogelaar, R., Martins, T.C., Sato, A.K., Iwao, Y., Gotoh, T., and Kagei, S. (2016). 3D reconstruction and multiple point cloud registration using a low precision RGB-D sensor. *Mechatronics*, 35, 11–22.

Tavares, R.S., Sato, A.K., Martins, T.C., Lima, R.G., and Tsuzuki, M.S.G. (2019). GPU acceleration of absolute EIT image reconstruction using simulated annealing. *Biomed Signal Proces*, 52, 445–455.

Ueda, E.K., Martins, T.C., and Tsuzuki, M.S.G. (2018). Planar curve fitting by simulated annealing with feature points determination. *IFAC-PapersOnLine*, 51, 290–295.

Zhao, F., Xu, X., and Xie, S. (2009). Computer-aided inspection planning—the state of the art. *Comput Ind*, 60(7), 453–466.